Journal of Applied Electrochemistry (2024) 54:1057–1073
https://doi.org/10.1007/s10800-023-02018-3

RESEARCH ARTICLE

Electrochemical perspective on the applicability of electroosmosis for clay consolidation

Yuri Sugiyama[1] · **Nagate Hashimoto**[2] · **Cyrille Couture**[1] · **Daiki Takano**[1]

Received: 21 August 2023 / Accepted: 29 October 2023 / Published online: 23 December 2023

Abstract

There are three main electrochemical factors affecting the electroosmotic flow in clay soil: the voltage loss at the clay/electrode interface, the type of current carriers in the soil, and the ion composition change in the clay due to voltage application. Appropriate evaluation of these factors is important to cost effectively implement electroosmosis for in situ soil consolidation projects. In this study, three different experimental systems were developed and used to investigate electrochemical reactions occurring in reconstituted and natural marine clay during electroosmotic consolidation. The results of polarization tests show that the voltage loss at the clay/electrode interface is different depending on the combination of the clay material and electrode material. The results of electroosmotic element test also show that electroosmotic dehydration does not increase if large current–voltage value is applied and that an optimal current–voltage value for causing electroosmosis depends on the cohesive soil composition. If the clay contains a lot of oxidizable ions, such as sodium, these ions affect electrophoresis and chemical reactions that occur in the soil. Therefore, the optimal configuration to apply electric current also differs depending on the clay. The results of laboratory-scale electroosmotic dehydration tests, arranged in a realistic in situ layout, are performed to study the relationship between soil dehydration, consolidation, and surface crack generation.

Graphical abstract

Keywords Electroosmosis · Dehydration · Polarization · Cohesive soil · Clay consolidation

✉ Yuri Sugiyama
sugiyama-yu@p.mpat.go.jp

Nagate Hashimoto
hashimoto-n-p@p.mpat.go.jp

Couture Cyrille
cyrille.couture-p@p.mpat.go.jp

Daiki Takano
takano-d@p.mpat.go.jp

[1] Soil Mechanics and Geo-Environment Group, Geotechnical Engineering Department, Port and Airport Research Institute, Yokosuka, Kanagawa 239-0826, Japan

[2] Materials Research Group, Structural Research Department, Port and Airport Research Institute, Yokosuka, Kanagawa 239-0826, Japan

1 Introduction

The use of electroosmosis in geotechnical and geo-environmental engineering has extensive application potential, such as soil consolidation and stabilization, strength improvements, soil remediation, and dewatering of sludge [1–12]. Xue et al. [2] examined the influence of electrode materials on the electroosmotic effect through electroosmotic experiments using various electrode materials. Ready et al. [3] examined the effectiveness of electroosmosis for dredged soil and found that the dehydration effect of electroosmosis is very high compared to mechanical dewatering, such as belt press. Zareh et al. [8] conducted electroosmotic consolidation test and unconfined compression test on naturally deposited clay and kaolin clay and showed that the higher the applied voltage, the larger the consolidation settlement, and the greater the strength of the specimens after electroosmosis. Although there have been many studies applying electroosmosis to clay, few studies have examined the electrochemical factors that affect the electroosmosis effect on clay. Soil consolidation is a phenomenon in which water contained between soil particles (pore water) dehydrates over time and increases in density, due to the application of an external load. Clay particles are often negatively charged in water. Therefore, during electroosmosis, the positively charged pore water near the surface of the soil particles flows toward the cathode side, causing a transient dehydration of pore water.

In the field of civil engineering, electroosmosis has been used as a rapid stabilization method when the embankment moved greatly during the dehydration of the cofferdam in Singapore [13]. In addition, field demonstration experiments using electroosmosis have been reported, such as soil improvement of soft soil [14] and dehydration of organic silty clay [15]. Additionally, field tests have been performed to determine the required parameters its potential application to other field applications [16–21]. Electroosmotic dehydration phenomenon in soils have also been investigated through analytical models [22–25].

Despite a few successful examples of applications in the field, the use of electroosmosis remains scare at the engineering scale. One of the reasons is that it remains difficult to determine the specifications for on-site application of the electroosmotic consolidation method. The electroosmotic effect depends on both the ground composition and the electrode material. Therefore, it is necessary to investigate the electroosmotic phenomenon in cohesive soil from an electrochemical point of view.

Two main electrochemical phenomena, electroosmosis and electrophoresis, occur by applying current to cohesive soil. Electrophoresis, in which ions and colloids act as current carriers, occurs simultaneously to electroosmosis when an electric potential is applied. Both ion migration (electromigration) and colloid migration (electrophoresis) will be referred to as "electrophoresis" without distinction. As mentioned above, cohesive soil is often negatively charged, which causes water to move toward the cathode due to electroosmosis. The electroosmotic consolidation method is a method to dehydrate cohesive soil using such movement of pore water. The electrochemical factors that affect the electroosmotic effect are (1) the voltage drop at the clay/electrode interface, (2) the type of current carriers in the soil, and (3) the ion composition change due to the applied electric potential.

Appropriate evaluation of these factors is important to assess the feasibility of using electroosmosis to consolidate and improve the mechanical properties of cohesive soil in the field. However, the effect of these factors on the electroosmotic effect remains poorly studied. The purpose of this study is to evaluate electroosmotic consolidation of cohesive soil, from an electrochemical point of view. In this study, we developed four different experimental systems and presented results for two investigated types of cohesive soils.

2 Materials and methods

2.1 Soil materials

In this study, kaolin clay and Tokyo Bay clay are used. Kaolin clay is reconstituted from a powder of 1:1-type layered silicate mineral in which Si–O tetrahedral layers and octahedral layers of O and four OH are coordinated around Al by sharing O. A kaolin slurry is initially prepared by adding tap water to the dry powder and stirring. In general, slurry samples are prepared with a water content of twice the liquid limit, so the initial water content in this study was set to 100%, twice the liquid limit of kaolin. Tokyo Bay clay is naturally deposited marine clay from the Tokyo Bay area. The initial water content was 140.6%, which is natural water content. The solution contained in the pores of the clay (hereafter referred to as pore water) is seawater. Table 1 shows the analysis results of the solution. From Table 1, it can be seen that the ionic strength is high, including calcium and magnesium ions. Anions were measured by ion chromatography, sodium and potassium by flame atomic absorption spectrometry, and calcium and magnesium by emission spectrometry. In addition, quartz, plagioclase, muscovite, chlorite, and pyrite were identified from X-ray diffraction (XRD) measurements of Tokyo Bay clay. Physical

Table 1 Tokyo Bay clay water composition

Cl	SO_4^{2-}	Na	K	Ca	Mg
7300	2000	4200	200	220	530

Unit: mg/L

Table 2 Physical properties of Tokyo Bay clay and Kaolin clay

	Kaolin	Tokyo Bay clay
Density (g/cm^3)	2.77	2.68
Liquid limit (%)	52.1	102.4
Plasticity index	22.4	63.1
Hydraulic conductivity (cm/sec)	6.3E-06	6.1E-07
D60 (mm)	0.0020	0.0046

properties of Tokyo Bay clay and kaolin clay are shown in Table 2. The plasticity index is an index that expresses the viscosity of clay, and the higher the plasticity index, the higher the viscosity. Moreover, both kaolin clay and Tokyo Bay clay have small permeability coefficients, and they are materials that require a long time for drainage.

2.2 Experimental setup

In this experimental campaign, three different types of apparatus were used to perform polarization tests and electroosmotic consolidation tests at the element scale, as well as a larger design scale representing an in situ field layout in a laboratory environment.

2.2.1 Polarization test apparatus

The clay/electrode interface reaction causes a rapid voltage drop at the interface [26, 27]. Therefore, voltage gradient at the clay/electrode interface is called voltage drop in this study. When the voltage drop increases, the voltage acting in the clay decreased, so electroosmotic dehydration hardly occurs and the volume of dehydration does not increase. The polarization value, an indicator of the voltage drop at the clay/electrode interface, is measured trough the polarization test.

For this set of experiments, Kaolin clay and Tokyo Bay clay were used as cohesive soil. Three types of electrode materials were used: stainless steel (SUS 304), aluminum (A5052P), and iron (SS400). A schematic view of the experimental equipment is shown in Fig. 1. The testing cell is 60 mm in diameter and 40 mm in height and filled with clay. A copper electrode was used as the counter electrode and a salt bridge was installed at a position about 1.5 mm away from the working electrode. The polarization values at the clay/electrode interface are measured, while a saturated silver-silver chloride electrode was used as a reference electrode. The internal aqueous solution is saturated with potassium chloride (KCl). The size of the working electrode is 1.0 cm^2.

For each test with different cohesive soil and electrode material, a voltage up to 5 V (vs. SSE) at 96 mV min^{-1} is

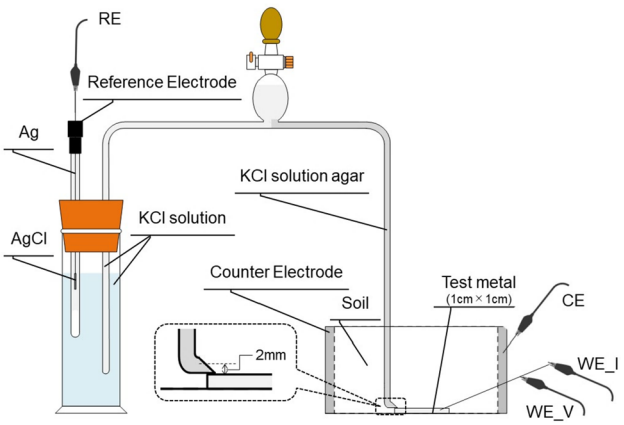

Fig. 1 Schematic view of the experimental equipment for measuring polarization values. The working terminal (WE_V), for voltage measurement, the working terminal (WE_I), for current measurement, the counter terminal (CE), and the reference terminal (RE) are identified

applied, while the polarization potential is measured. Comparison of the experimental results using new electrodes with those using reused electrodes showed differences in dewatering rate and final dewatering volume. This suggests that the corrosion of the electrode causes a larger voltage loss at the clay/electrode interface and therefore a smaller voltage acting on the entire clay. To reproduce the same initial condition and avoid corrosion effect, new electrodes are used for each experiment. Since the drain material is filled with water in the in situ soil consolidation and the voltage loss due to corrosion may be smaller, the effect of voltage loss is expected to be larger in the experiment.

2.2.2 Electroosmotic element testing apparatus (1D)

Dehydration tests using electroosmotic consolidation test apparatus were carried out on Kaolin clay and Tokyo Bay clay in order to investigate current carriers in the clay and changes in ion composition in the clay due to voltage application.

Sugiyama et al. [28] performed an Electron Probe Micro-Analyzer (EPMA) on kaolin specimens after electroosmotic consolidation tests and clarified that the ion distribution of pore water in Kaolin clay became almost uniform. On the other hand, Tokyo Bay clay contains many ions in its pore water from the marine environment where it was saturated. To investigate the ion distribution of pore water in Tokyo Bay clay specimen, the ion distribution of the cross section of the surface of a specimen was analyzed by EPMA.

A series of experiments were performed using an electroosmotic consolidation test apparatus. A schematic diagram of the test equipment is shown in Fig. 2. In order to investigate the consolidation characteristics of clay soil by electroosmosis, a new apparatus was designed to meet

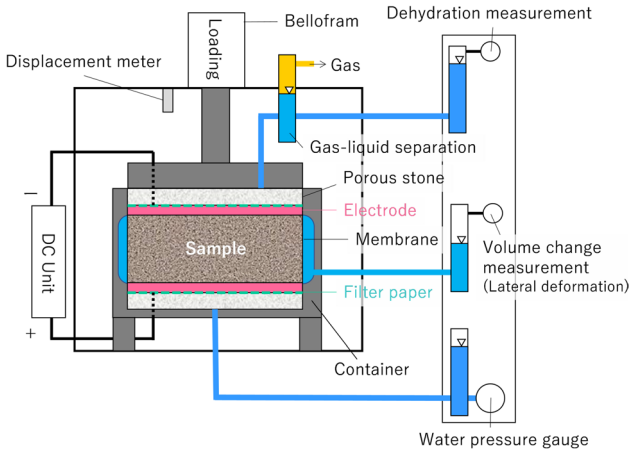

Fig. 2 Schematic view of the Electroosmotic element testing apparatus

the same requirements as the standard consolidation test apparatus [29]. A direct current is applied between the upper and lower end surfaces of the specimen in contact with the electrodes. A gas–liquid separator is installed to separate the gas, generated by the electrode reaction, and water, dehydrated by electroosmosis. In addition, multiple holes with a diameter of 3 mm were drilled in the electrode so that the gas generated by the electrode reaction would not stay between the electrodes and the clay. The effective electrode area in contact with the clay sample is 2,239 mm^2, equivalent to 80% of the total surface area. Furthermore, lateral deformation can be measured since the specimen shrinks due to electroosmosis. The size of the slurry specimen was 60 mm in diameter and 20 mm in height, as in the standard consolidation test, so the initial electrode spacing was 20 mm. The electrode spacing become narrower as the vertical deformation of the specimen induced by electroosmotic dehydration. But the vertical deformation during the test was less than 1 mm, confirming that the electrode spacing remained almost constant during the test. The test was performed applying a vertical load equal to the lateral confining pressure. Vertical load is applied so that the electrodes are always in contact with the clay edge surface even during consolidation settlement. Since electroosmotic consolidation causes the specimen to shrink, a membrane is installed to prevent drainage from the side of the specimen and a lateral pressure equal to the vertical load is applied. The gap between the membrane and the consolidation container is filled with water. The lateral pressure is equal to the water pressure filled in the gap, and the water pressure is equal to the difference in water head between the water tank and the consolidation container installed next to the consolidation test apparatus. The results of the tests, in which only vertical and lateral loads were applied for a certain period of time, confirmed that the effect of these loads on electroosmotic consolidation was very small.

After the experiment, post-consolidation surface analysis was conducted using an EPMA apparatus.

An electron probe micro-analyzer JXA-8200 manufactured by JEOL Ltd. was used for the analysis. The analysis conditions were an acceleration voltage of 15 kV, a sample current of 200 nA, a probe diameter (the diameter of the electron beam incident on the sample) of 50 µm, and a pixel size (the size of one section to be analyzed) of 100 µm. For the analyses, specimens with a length of 1.5 cm, a width of 5.5 cm, and a thickness of about 0.5 cm were obtained by cutting the specimen near the center with a cutter and vacuum drying for one week. After embedding it in resin, the analysis surface was coated with carbon to provide electrical conductivity and EPMA analysis was performed according to JSCE-G574 [30]. The proportion method is used for conversion of concentration, and although the relative concentrations of the measured elements can be compared, it is generally considered that absolute values cannot be guaranteed. However, according to an example of measurement of a sample in which chloride ions are mixed in ordinary cement, the mass concentration obtained by this method corresponds to the data obtained by chemical analysis, and the absolute value also has a certain degree of accuracy. The condition for creating the surface analysis image was to display pixels excluding insubstantial parts, such as air gaps.

2.2.3 3D model test-scale electroosmotic apparatus

For on-site application, in order to examine the three-dimensional effect of electroosmotic dehydration, with an electrode placement similar to potential in situ layouts, experiments were conducted inside an acrylic cylindrical model soil tank.

Kaolin clay with an initial water content of 100% was used as the soil material. The tank is an acrylic cylindrical container with an inner diameter of 410 mm and a height of 440 mm. A hollow cylindrical rod with an outer diameter of 56 mm and a thickness of 2 mm is placed in the center of the thank and acts as the cathode material. Multiple holes with a diameter of 2 mm are drilled in the rod to drain water accumulating at cathode during the test. A permeable fabric was wrapped around the surface of the cathode and a tube was passed through the center of the cathode to a height of 10 mm from the bottom of the ground to remove water at the bottom of the drain.

A Kaolin clay slurry, with a water content of 100%, is poured into the tank to a height of 270 mm. To perform image analysis, a surface texture contrasting with the white color of the clay is created by coating the sides of the acrylic container with colored Kaolin, black beads are randomly sprinkled over the top surface of the clay. Three anodes of

φ12 mm are installed around the cathode so that the distance between anode and cathode is 110 mm. Figure 3 summarizes the experimental cross-sections. Three cases (Case Al-Al_12, Case Al-Al_6, Case Al-Fe_12) were conducted to examine the differences in the cathode material and the difference in the anode surface area. In Case Al-Al_12 and Case Al-Al_6, aluminum was used as the electrode material for both the cathode and anode. In Case Al–Fe, the cathode material was iron and the anode material was aluminum. In Case Al-Al_12, three anodes of φ12 mm were used. In Case Al-Al_6, three anodes of φ6 mm were used in order to evaluate the effect of the anode surface area on the volume of dehydrated water. In all cases, a constant current of 0.4 A was applied for 20 h. The maximum voltage is 73.5 V.

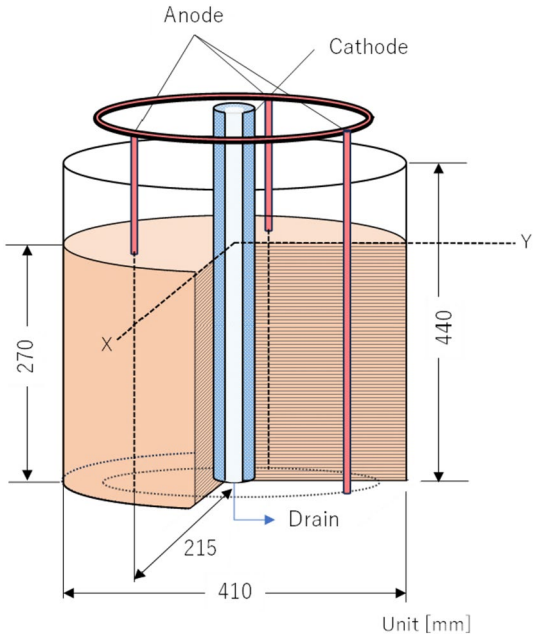

Fig. 3 Schematic view of the 3D model test-scale electroosmotic apparatus

3 Results

3.1 The polarization test

The polarization curves are shown in Fig. 4. The vertical axis indicates the amount of polarization, where the positive side of the vertical axis is the anode side, and the negative side is the cathode side. The amount of polarization was obtained by subtracting the spontaneous potential from the measured potential. The polarization on the anode side was lower for aluminum and iron than for stainless steel, in the case of Kaolin clay, as shown in Fig. 4a. In the case of stainless steel, the polarization on the anode side changes rapidly at a current density of 0.2 mA cm^{-2}. The polarization on the cathode side was almost the same for all materials, but the polarization curve of aluminum changes rapidly at a current density of 0.5 mA cm^{-2}. In the case of Tokyo Bay clay, as shown in Fig. 4b, the polarization curve on the anode side changes rapidly at a current density of around 5.0 mA cm^{-2} with stainless steel and iron. There was also no significant difference between materials in the polarization curve on the cathode side.

3.2 Electroosmotic element test

3.2.1 Kaolin clay

Separate experiments were conducted for three constant current values of 0.01 A, 0.02 A, and 0.05 A. In all experiments, the electrodes are aluminum for the anode material and iron for the cathode material. Figure 5 shows the test results. The final dehydration amount was the smallest when the constant current value was 0.01 A, and the dehydration curves of

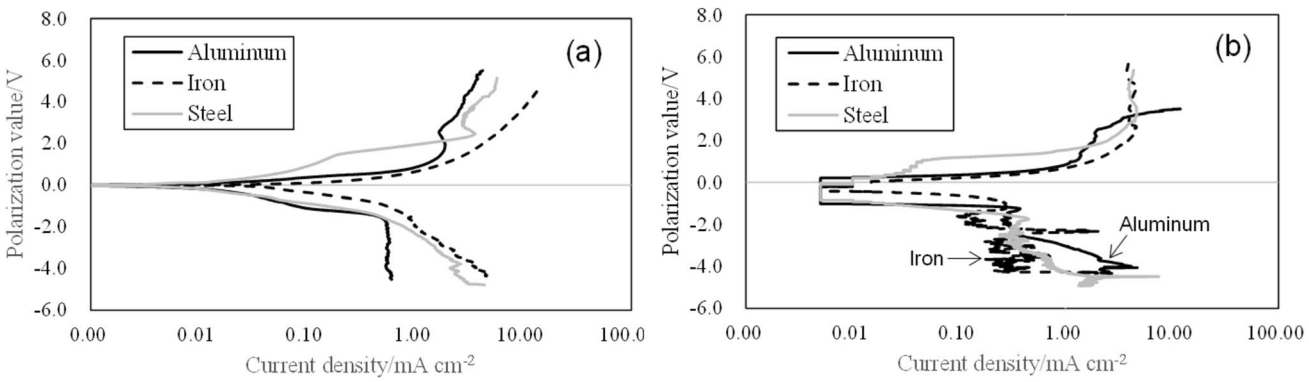

Fig. 4 Polarization curves of Kaolin clay (**a**) and Tokyo Bay clay (**b**). The negative values are for the cathode and the positive values are for the anode

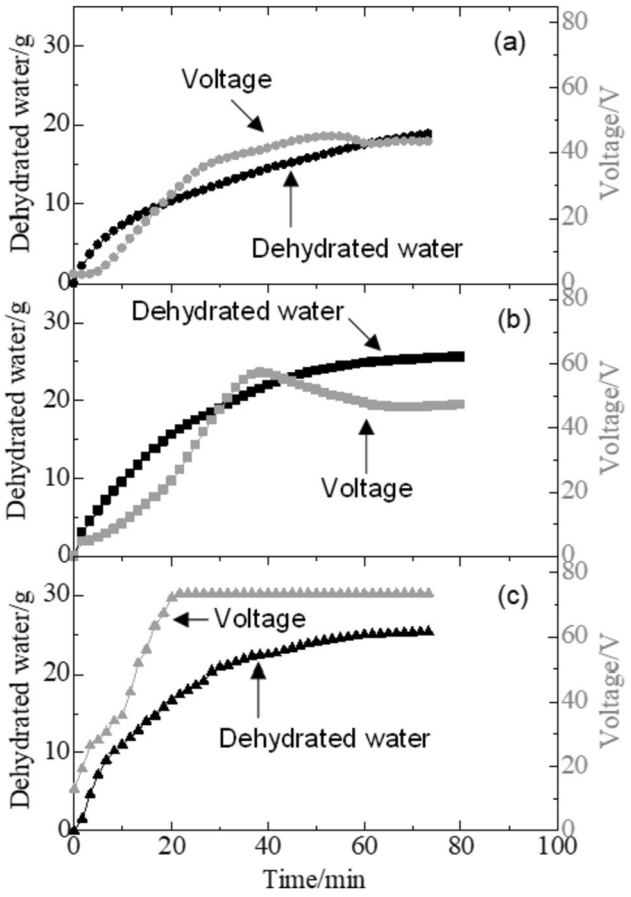

Fig. 5 The relationship between dehydrated water and voltage over time in case of Kaolin clay. The result of Case 0.01 A (**a**), Case 0.02 A (**b**), and Case 0.05 A (**c**)

the cases of 0.02 A and 0.05 A are almost identical. The dehydration rate just after applying current was almost the same regardless of the constant current value. In the case of 0.01 A, indicated by the black line, the amount of dehydration increases as the voltage potential increases gradually. However, when the voltage value exceeded 40 V, the voltage became constant and the final voltage value was smaller than the final voltage value of 73.5 V in the cases of 0.02 A and 0.05 A. The final dehydration volume was smaller since the voltage acting on the cohesive soil was lower than that in other cases. Seeing the change in the potential with time at 0.05 A indicated by gray line in Fig. 5c, the potential rises quickly. From the polarization curve shown in Fig. 4a, when iron is used on the cathode side, the amount of polarization increases when the current density exceeds 0.8 mA cm^{-2}. When aluminum is used on the anode side, the amount of polarization increases sharply when the current density exceeds 1.0 mA cm^{-2}. In the cases of 0.02 A and 0.05 A, the current densities are about 0.7 mA cm^{-2} and 1.8 mA cm^{-2}, respectively. The current density in case of 0.05 A is greater than the current densities at which the voltage loss rapidly increases. From these results, it is likely that much of the voltage measured in the 0.05A case was consumed by voltage losses and the actual voltage gradient acting in the clay was small. Therefore, almost no difference occurred between in these two dehydration curves. The average water content after the experiments were 0.01 A:53.8%, 0.02 A:50.6%, and 0.05 A: 49.6% and a high dehydration effect was obtained in all cases.

3.2.2 Tokyo Bay clay

The Tokyo Bay clay contains NaCl in the pore water, so the resistance of the clay is small. Therefore, the electroosmotic dehydration would take a long time if a constant current was applied, as in the case of Kaolin clay. Considering that energization under constant voltage condition is effective, experiments were performed at constant current condition and constant voltage condition. In Case CC-Al, both electrodes were made of aluminum and the experiment was conducted under a constant current condition of 0.05 A. In Case CV-Fe, aluminum was used for the anode, iron was used for the cathode, and the experiment was conducted under constant voltage condition. The constant voltage value was increased stepwise in the order of 10 V → 20 V → 40 V → 73.5 V, when the current value dropped to 0.1 A. Figure 6 shows the change in amount of dehydration and voltage over time. Comparing Case CC-Al, at a constant current condition of 0.05 A, in Fig. 6 and the result of Kaolin clay, at a 0.05 A constant current condition, in Fig. 5c, the potential of Tokyo Bay clay was very small and hardly changes until 400 min after applying current. Although the amount of dehydration gradually increased by electroosmotic dehydration even at a low potential, the dehydration time significantly increases. Figure 7 shows the relationships between energy consumption and dehydrated water. At the point indicated by the arrow in Fig. 7, the amount of dehydration is 20 g in both cases when the energy consumption is 12 kJ. Moreover, total dehydration was higher in Case CV-Fe energized under CV conditions, even though the final energy consumption was the same in both cases. Comparing the energy consumption to obtain the same amount of dehydration, it seems like that the dehydrate efficiently is higher in Case CC-Al than Case CV-Fe, but the time required for dehydration up to this point was 400 min in Case CC-Al, which is longer than the 180 min required to obtain the final dehydration amount of 27 g in Case CV-Fe. Comparing the time required to reach the same amount of energy consumption and dehydration shown by the arrows in Fig. 7, it is clear that Case CV-Fe dehydrates 6 times faster than that in Case CC-Al. A comparison of the time required to reach dehydration amount of 20 g, which is the final dehydration in Case CC-Al, resulted in three times faster dehydration time in Case CV-Fe. The average water content after experiments were 73.9% for Case

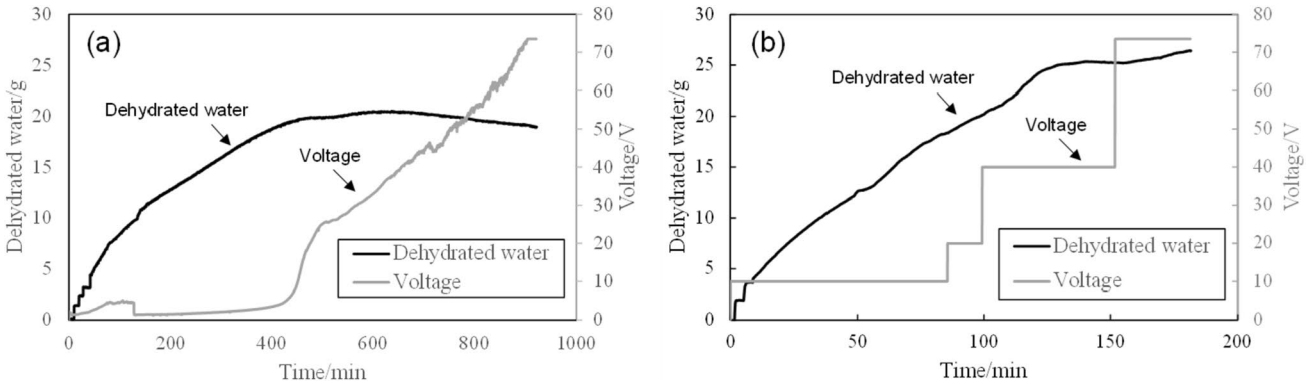

Fig. 6 The relationship between dehydrated water and voltage over time in case of Tokyo Bay clay. The results of Case CC-Al (**a**), and Case CV-Fe (**b**). The black line indicates changes in the amount of dehydration, and the gray line indicates voltage changes

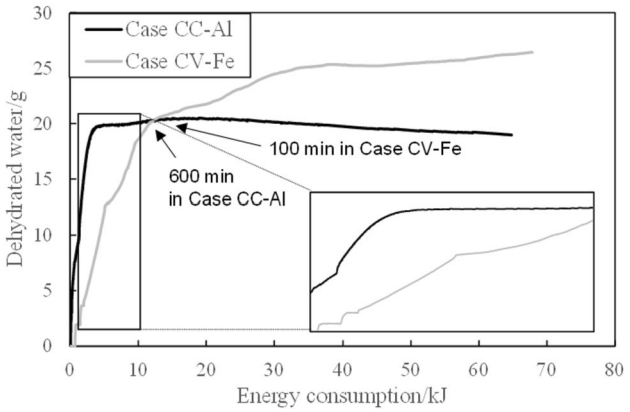

Fig. 7 The relationship between energy consumption and dehydrated water of Tokyo Bay clay. The black line indicates the result in Case CC-Al and the gray line indicates the result in Case CV-Fe

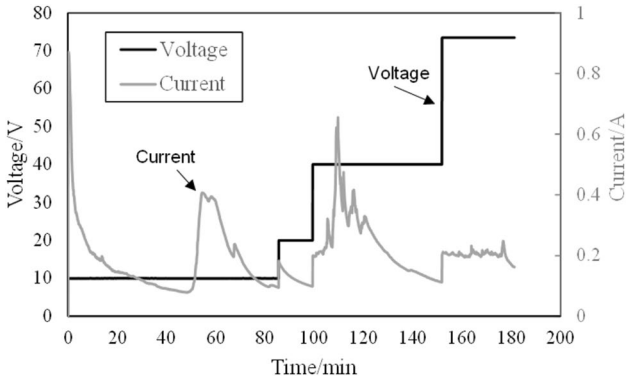

Fig. 8 The relationship between current and voltage over time of Tokyo Bay clay (Case CV-Fe). The black line indicates current changes and the gray line indicates voltage changes

CC-Al and 55.6% for Case CV-Fe. This value is below the plastic limit of Tokyo Bay clay in Case CV-Fe. From these results, the applying current under constant voltage condition is effective for electroosmotic dehydration of marine clay. It took 180 min to dehydrate the Tokyo Bay clay in Case CV-Fe, which is very short as a dehydration time for cohesive soil.

According to the change in current and voltage over time in Case CV-Fe, the current value increased sharply after 50 min, even though the voltage did not change (Fig. 8). Vertical displacement was measured in this experiment, and when the current increased rapidly, upward vertical displacement, i.e., displacement of the electrode away from the clay, occurred. However, when the container was lightly vibrated with a hammer, it was observed that large bubbles were released into the gas–liquid separator. At this time, the current gradually decreased and the vertical displacement returned to normal state. Therefore, it is considered that the gas generated by the electrode reaction was temporarily trapped between the specimen and the electrode, causing the current value to increase suddenly. In this experiment, immediately after increasing the voltage value, the current value was checked, and if necessary, the container was degassed by vibrating it. The rapid change in the current value is associated with the degassing.

3.3 EPMA results of Tokyo Bay clay

EPMA analysis was performed on the specimen after the experiment reported in Sect. 3.2.2. The elements measured were silicon (Si), aluminum (Al), calcium (Ca), magnesium (Mg), and chlorine (Cl). The analysis results of Case CC-Al and CV-Fe are shown in Fig. 9I and II, respectively. Figure 9a is a photograph of the analyzed surface after vacuum drying, and Fig. 9b shows the concentration distribution of each element. The top is the cathode side of the sample, and the bottom is the anode side. The scale on the left side of each image represents the depth from the top, and the interval between the scales is 1 mm. Since

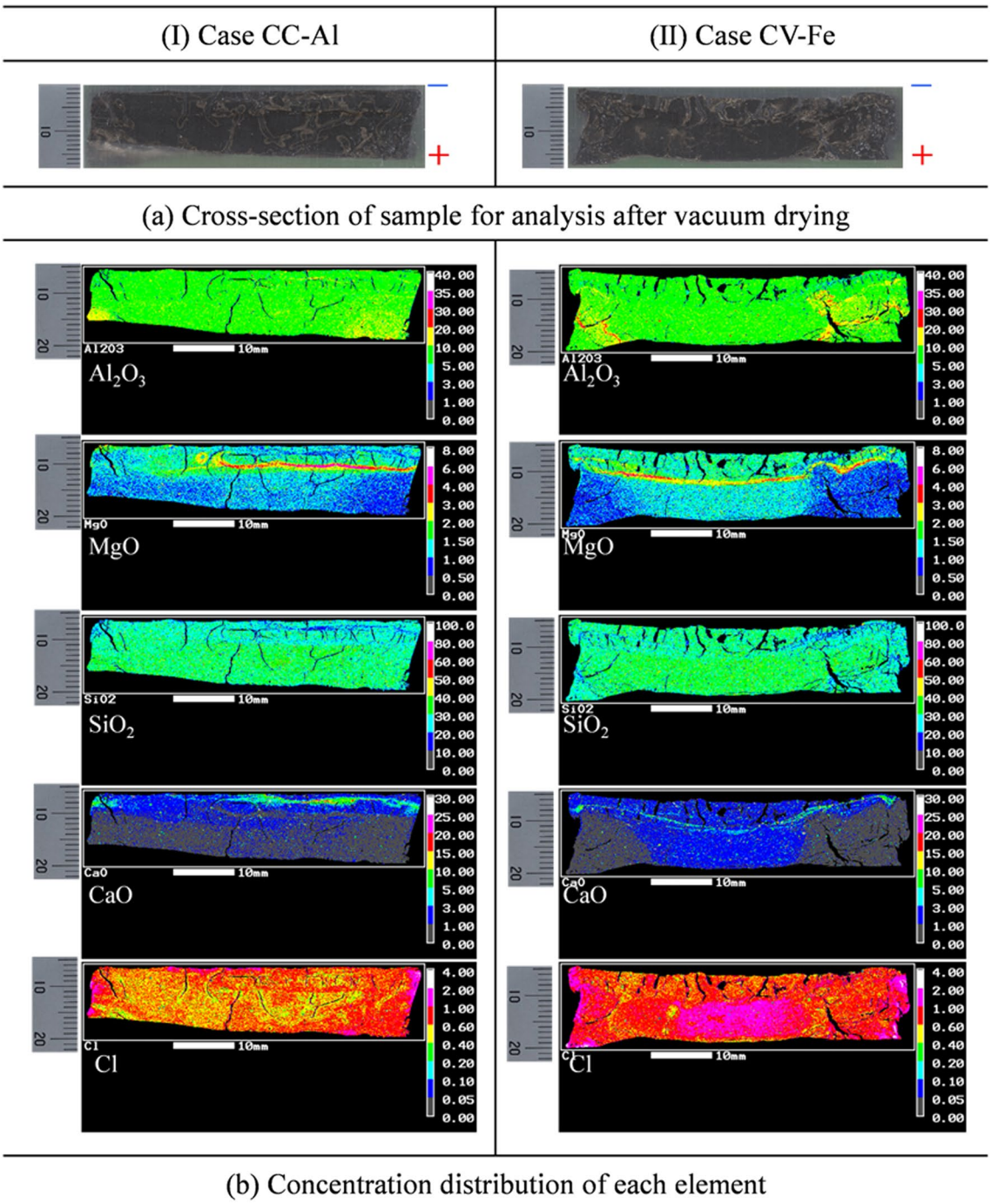

Fig. 9 EPMA analysis results of constant current (Case CC-Al) and constant voltage (Case CV-Fe)

the resin used for embedding contains Cl, the concentration distribution of Cl is only for reference. In Fig. 9I-a, horizontal cracks can be observed at a distance of 6 mm from the top of the sample, and multiple vertical cracks are present throughout the specimen. As shown in Fig. 9I-b, the Al_2O_3 concentration is almost constant, except for a slightly higher concentration at the left and right sides of the bottom of the sample. The MgO concentration is high at a depth of about 3 mm from the top in the 2/3 region of the right side of the sample surface. The SiO_2 concentration is low at a depth of about 2 mm from the top, but the rest was generally constant. The CaO concentration is high from the top of the sample to a depth of about 3 mm, and the surrounding area was slightly higher. The concentration over the rest of the sample is generally constant. The Cl concentration is particularly higher in some areas on

the outer periphery of the analyzed surface than inside of the specimen.

Next, as shown in Fig. 9II-a, there is almost no difference between Case CC-Al and CV-Fe in terms of the condition of analysis surface. The MgO concentration was low in the lower left and lower right and a high layer was seen at a depth of 0 to 7 mm from the upper part. The position of its high layer is lower than that in Case CC-Al.

3.4 Qualitative analysis of dehydrated water by electroosmosis

In the electroosmotic dehydration test using Kaolin clay, the dehydrated solution was colorless and transparent. While the dehydrated solution from Tokyo Bay clay was dark brown. When the pH of the water was measured, both were highly alkaline, around pH 14.0. It is caused by OH- ions being released from the cathodic reaction at the cathode. To investigate the ions that caused the coloration of the dehydrated solution from Tokyo Bay clay in the Case CC-Al experiment, quantitative analysis and qualitative analysis were performed for 6 cations and 7 anions.

After filtering the sample with a 0.45-μm PTFE membrane filter, cations were quantitatively analyzed by ion chromatography for $Ca2^{+}$, Na^{+}, and $Mg2^{+}$ and phenanthroline absorptiometry for $Fe2^{+}$. The analysis was performed according to JIS K 0102:2019 [31]. Colorimetric method by dipyridyl method is used for quantitative analysis of $Fe2^{+}$ and total iron ions ($Fe2^{+} + Fe3^{+}$), and $Fe3^{+}$ is determined from the difference. $Al3^{+}$ was analyzed by quantitative determination (in terms of Al) by atomic absorption spectroscopy as shown in the Standard Methods of Analysis for Mineral Springs [32]. For anions, the presence or absence of anions was determined by checking the retention time of each anion standard solution and the chromatogram of the sample test solution. For anions that may be contained, semi-quantitative values were calculated from the electrical conductivity ratios of the standard solution and the sample test solution. The chromatograph anion qualitative analysis was performed using an ion chromatograph analyzer manufactured by Thermo Fisher Scientific (DIONEX INTEGRION HPIC system IonPac AS22, IonPac AS18).

Table 3 shows the results of anions obtained by quantitative analysis and cations obtained by qualitative analysis. The semi-quantitative values are calculated from the relative area ratio obtained from the electrical conductivity of the standard substance and the sample solution and do not guarantee the accuracy of the absolute values. From these results, the content of ions that may affect coloration is very small and that the ions contained in the solution are not the cause of the reddish brown color of the solution. The solution is drained from the cathode side and has a very high pH. In this case, it is assumed that the zeta potential is the largest

Table 3 Anions and cations in Tokyo Bay clay dehydrated water (Unit: mg L^{-1})

Anions component	
Ca^{2+}	< 1
Na^{+}	8600
Fe^{2+}	< 4
Fe^{3+}	< 4
Mg^{2+}	< 1
Al^{3+}	< 100
Cations component	
F^{-}	0.3
Cl^{-}	90
NO_2^{-}	0.1
Br^{-}	0.3
NO_3^{-}	0.2
SO_4^{2-}	39

"<" indicates less than the lower limit of quantitation

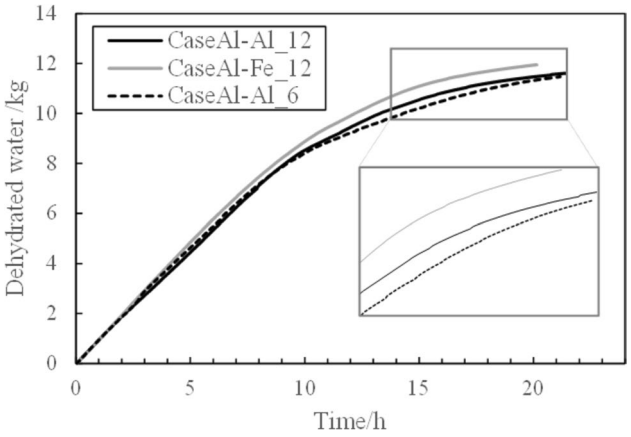

Fig. 10 The relationship between dehydrated water and time for all cases. The black, gray, and black-dashed lines indicate the results for Case Al-Al_12, Case Al-Fe_12, and Case Al-Al_6, respectively

value that the clay has. In addition, the solution was stand for a long time without precipitation, and the color of the solution did not change. Therefore, the color is considered to be that of a colloidal solution in which the fine particles of clay are dispersed.

3.5 3D model test-scale electroosmotic dehydration test

Figure 10 summarizes the relationship between dehydrated water and time for all three cases. The amount of dehydration was the largest in Case Al-Fe_12 with iron cathode, see Fig. 10. Comparing the results of Case Al-Al_12 and Case Al-Al_6, the dehydration curves are almost the same. The current densities are 1.3 mA and 2.6 mA for the φ12 mm and φ6 mm cases, respectively, and the polarization curves in Fig. 4 show that the amount of polarization is similar

for both cases. From these results, the difference in anode surface area has not significant effect on the dewatering rate and final dewatering volume in this experiment.

Figure 11 shows the results of image analysis performed using images taken with a lateral camera in order to compare the amount of settlement in Case Al-Al_12, Case Al-Al_6, and Case Al-Fe_12. The amount of settlement near the cathode and at the monitoring point is different because the clay surface near the cathode is detached from the electrode at an earlier stage. Therefore, a settlement change as shown in Fig. 11 is at a monitoring point. The analysis was performed until the dehydrating clay started to contract laterally and separated from the wall surface. The final ground heights are similar for Case Al-Al_12 and Case Al-Al_6. The shrinkage was occurred faster in Case Al-Al_12 than Case Al-Al_6. The amount of total settlement was the largest in Case Al-Fe_12, and the clay started detaching from the outer wall at a later time. In Fig. 10, the dehydration curve of Case Al-Fe_12 begins to differ from the other two cases after 600 min (10 h). In addition, there is a difference in the dehydration curve between Case 1 and Case 1t after 700 min (11–12 h). These times coincide with the times at which deformation due to shrinkage begins to dominate over settlement (Fig. 11).

Figure 12 shows a surface color map of deviatoric strain concentration obtained from digital image correlation (DIC) at different stages of the experiments. The time stamps in Fig. 12 are identified on the settlement curves in Fig. 11. The circular cracks labels in the figure identify cracks that occur concentrically to the central cathode rod, and the radial crack identify crack that occur from the cathode toward the anode. Comparison of DIC results with crack observations shows that cracks occur where deviatoric strain increases. The circular cracks occurred around the cathode at time No.1 in Fig. 12a-Case Al-Al_12. After that, circular cracks expanded from the cathode side to the anode side, and these were generated in such a way that the anode separated from the clay at time No.2. Radial cracks were observed to extend gradually from the cathode to the anode. Circular cracks were generated connecting the anodes, and three large radial cracks generated from the cathode to the anode at time No.3. There is almost no change in the area targeted for image analysis at time No.4, the whole clay between the cathode and the anode began to shrink as if lifted, and countless circular cracks occurred between the anode and the wall. Similar tendency was obtained in Case Al-Fe_12. However, circular cracks developed faster than radial cracks in Case Al-Al_12, and radial cracks developed faster than circular cracks in Case Al-Fe_12. On the other hand, in Case Al-Al_6, a circular crack occurred around the cathode, but the circular crack connecting the anodes did not occur as in the other two cases. Shrinkage occurred like that in the clay blocks separated by three large radial cracks peeled off from the cathode. Comparing the results of Case Al-Al_12 and Case Al-Al_6 reveals that anode surface area affects the ground deformation during electroosmosis dehydration. When the electrode of φ12 mm is used, circular cracks grow faster than radial cracks. On the other hand, when the electrode of φ6 mm is used, radial cracks extend faster than circular cracks.

Due to the cracks, the clay on the ground surface around the cathode gradually peeled off from the cathode. In addition, due to the detachment, deformation such as swelling occurred near the center of the cathode. At this time, settlement due to self-weight consolidation also occurred at the same time, and it was confirmed that the dehydrated water accumulated on the ground surface along the wall surface. After 10 h from the start of experiment, three of the cracks formed on the cathode became large cracks extending to the wall surface. After the crack reached the wall surface, it was confirmed that the water accumulated on the ground surface near the wall surface was dehydrated, and deformation due to contraction rather than settlement due to electroosmotic dehydration was dominant. Regarding the crack generation, all cases showed the same tendency. After numerous fine cracks were generated around the cathode in the initial stage, three of them became large cracks extending to the vicinity of the wall surface. The angular interval between the

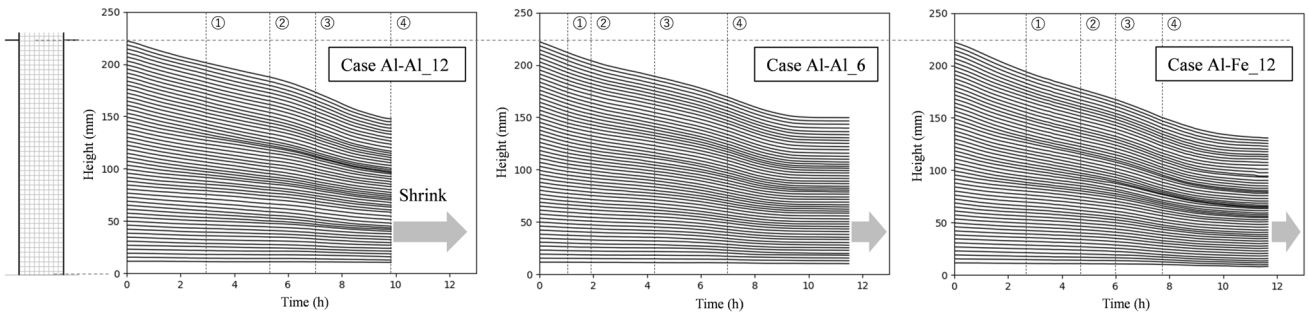

Fig. 11 The results of image analysis performed using images taken with a lateral camera in order to compare the amount of settlement in Case Al-Al_12, Case Al-Al_6, and Case Al-Fe_12

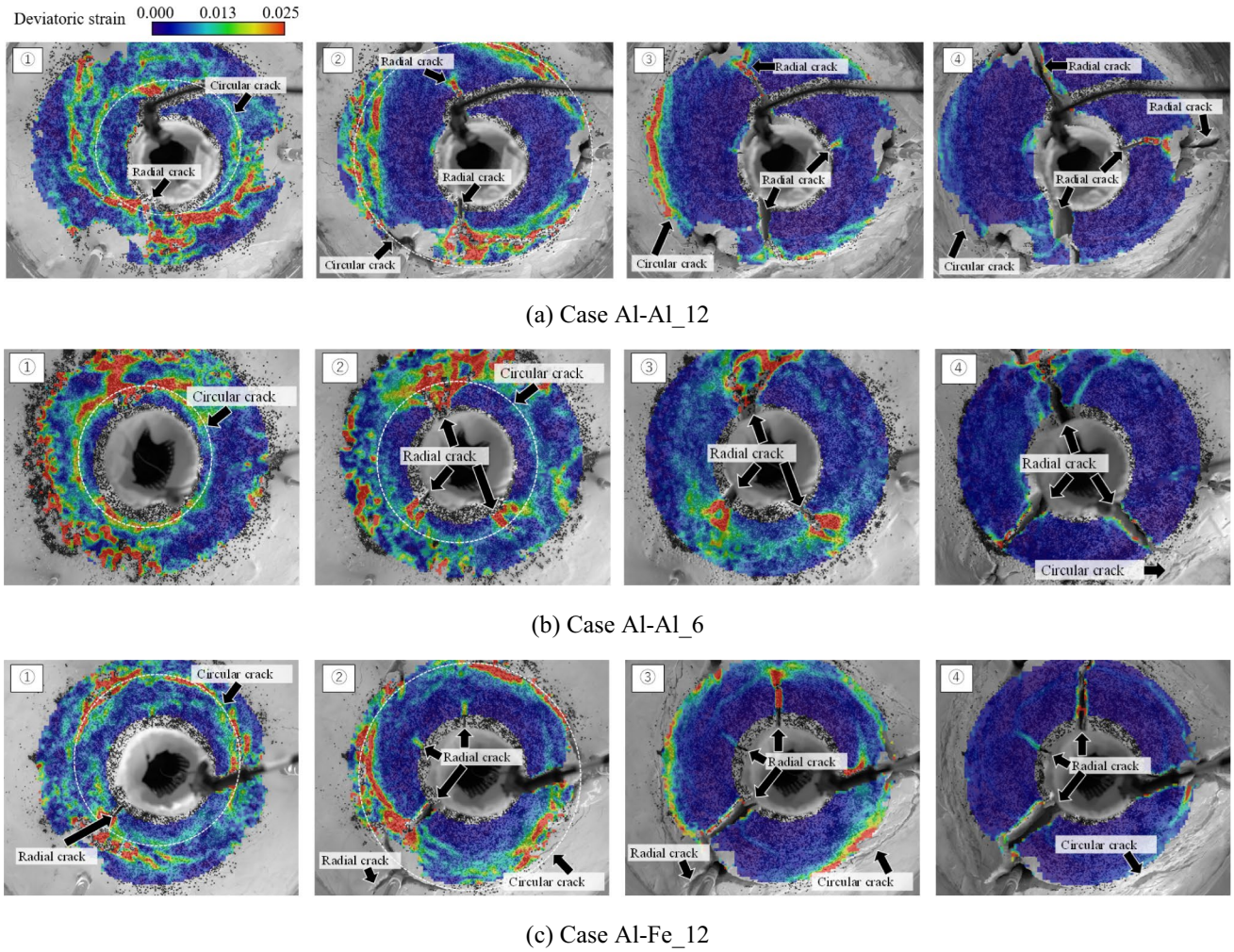

Fig. 12 Crack generation observed from the deviatoric stress distribution on the ground surface in (**a**) Case Al-Al_12, (**b**) Case Al-Al_6, and (**c**) Case Al-Fe_12

three major radial cracks occurred in the range of 100 to 140 degrees in all cases.

The water content was measured at the end of the experiment at four different sampling locations: (1) near the cathode, (2) near one of the anodes, (3) near the outer cylindrical wall, and (4) midway between the cathode and anode. At each location, clay samples were retrieved at every 20-mm height increments. Since the ground level was lower near the cylindrical wall compared to the central location near the cathode, the water content was measured up to a ground height of 60 to 80 cm. The results for the three experiments are shown in Fig. 13. In all cases, the water content of the model ground decreased from an initial value of 100% to less than 52%, which is the liquid limit of Kaolin. The average water content of the entire model ground in each case was 47.5% for Case Al-Al_12, 48.6% for Case Al-Al_6, and 46.0% for Case Al-Fe_12. The water content was lower in the experiment with iron material and lower in the experiment with aluminum material. At the measurement location between the anode and cathode, the water content was almost the same in the three cases study. This corresponds to the descending order of the final dehydration amount shown in Fig. 10. Regarding the depth distribution of the water content, the ground between the cathode and anode is lower at the bottom than at the surface. The water content is lower in the bottom part because the amount of dehydration due to self-weight consolidation is larger.

The only difference between Case Al-Al_12 and Case Al-Fe_12 is whether the cathode material is aluminum or iron, but there is a difference in the final dehydration amount. Figure 14 shows the results of potential measurement by a reference electrode placed at the boundary between the cathode and the clay in Case Al-Al_12 and Case Al-Fe_12. From Fig. 14, the larger potential is acting on the clay/electrode interface in Case Al-Al_12 than in Case Al-Fe_12. Due to the applied current, the water solution near the cathode

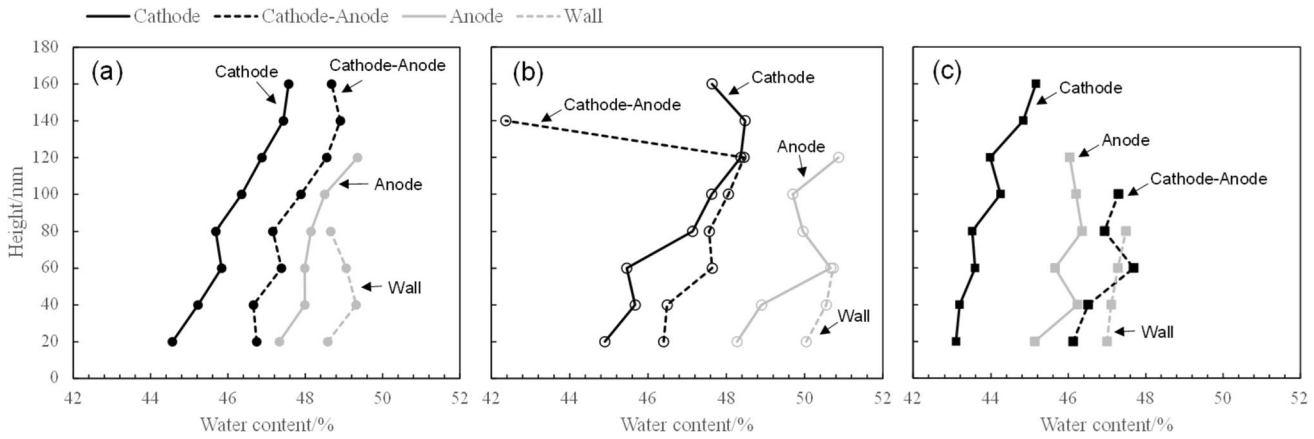

Fig. 13 The results of water content sampled at 4 locations and regular height intervals in the ground after the experiment in (**a**) Case Al-Al_12, (**b**) Case Al-Al_6, and (**c**) Case Al-Fe_12

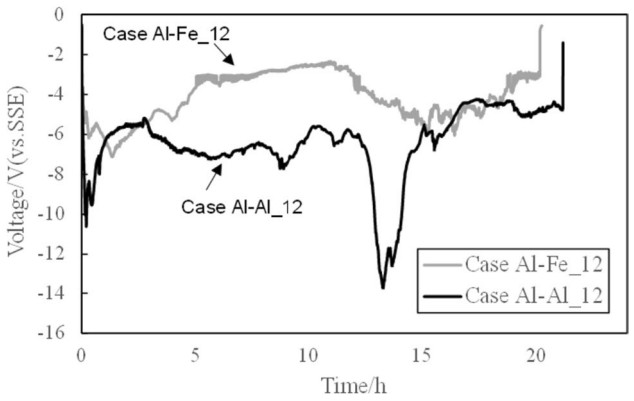

Fig. 14 The results of potential measurement by a reference electrode placed at the boundary between the cathode and the clay in Case Al-Al_12 (black line) and CaseAl-Fe_12 (gray line)

becomes alkaline (ph ≈ 14.0) and therefore creates favorable conditions for corrosion to occur at the surface of the aluminum rod. Conversely, iron greatly reduced corrosion because it is in an anticorrosive state in an alkaline environment. This is the reason for the difference in potential, acting on the clay/electrode interface, between iron and aluminum at the cathode.

The potential rises sharply 800 min after the start of the experiment. A voltage of 12 V is too large for the current density because hydrogen is generated if an electrochemical reaction occurs. Since the position of the reference electrode is below the water level, electric current can always flow. The reason for the sudden rise and fall in the voltage drop seen at 13–14 h is not clear. However, since dehydration was almost completed at this time, it did not affect dehydration.

From these results, it was revealed that when the circular cracks grow faster than the radial cracks, the time it takes for the clay to peel off from the wall and start shrinking becomes shorter. Conversely, when the radial cracks were extended faster than the circular cracks, the clay were significantly peeled off from the cathode. The effect of peeling off due to shrinkage appears in the distribution of water content as shown in Fig. 13. The upper part of the clay layer near the cathode in Case Al-Al_6 has a higher water content than the other cases because the clay peeled off from the cathode significantly. And the water content from the anode to the wall surface is also higher because the shrinkage that would cause the clay to peel off from the wall does not occur. On the other hand, in Case Al-Al_12 and CaseAl-Fe_12, which shrinks as if peeling from the wall, the water content from the anode to the wall was almost the same as the water content between the cathode and the anode. From the results of Case Al-Al_12 and Case Al-Al_6, the thickness of the anode affects the growth of circular cracks and that the smaller the anode diameter, the less circular cracks occur.

4 Discussion

To improve current methods and guide electroosmotic dehydration applications for ground, we discuss the effects of electrochemical factors on the electroosmotic effect based on the experimental results obtained in the current study.

4.1 Voltage drop at clay/electrode interface

During electroosmotic consolidation, a voltage of several tens of volts is usually applied between electrodes, so the current density of the electrodes gets large, and depending on the electrodes used, the voltage drops at the clay/electrode interface become large. Therefore, it is important to measure the voltage drop at the clay/electrode interface using a polarization test to understand the electrochemical

properties of the electroosmotic consolidation system. We conducted a voltage drop measurement test at the clay/electrode interface using two types of clay samples with different liquid resistance values and showed that even with the same electrode material, the trend observed in the polarization curve differs depending on the clay composition. When a saturated soil with high liquid resistance such as Kaolin clay is subjected to electroosmotic current, a large voltage difference can be applied to the clay between the electrodes using a relatively small current density. Therefore, the effect of the voltage drop, at the clay/electrode interface, has a limited effect on the electroosmotic dehydration. On the other hand, when using soil materials with low liquid resistance, such as Tokyo Bay clay, it is necessary to increase the current density in order to apply a large potential to the soil between the electrodes. In this case, the voltage drop at the clay/electrode interface has a large effect on the electroosmotic dehydration. Therefore, in this case, it is important to select an electrode material with a small voltage drop.

4.2 Current carriers in cohesive soil

The results of the electroosmotic consolidation test revealed that there is an optimal current value for each cohesive soil to induce electroosmosis. Figure 15 shows an equivalent circuit in clay soil to which a voltage is applied. There are two types of currents caused by the simultaneous effect of electroosmosis and electrophoresis. The measured current is expressed by the following equation.

$$I_m = i_{os} + i_{ph} \tag{1}$$

here, I_m[A] is the current measured by the ammeter, i_{os} and i_{ph} [A] are the current induced by electroosmosis and electrophoresis, respectively. The values of i_{os} and i_{ph} differ depending on the cohesive soil, so it is important to understand the ratio over I_m for electrochemical interpretation. There are various ways to arrange i_{os} and i_{ph}. In the current study, the value is obtained by dividing the applied voltage V by Eq. (2) such that

$$V = I_m\left(R + R_{in}\right) \Leftrightarrow \frac{V}{I_m} = \frac{1}{\left(\frac{1}{R_{os}} + \frac{1}{R_{ph}}\right)} + R_{in} \tag{2}$$

where R_{os}, R_{ph}, and R_{in} [Ω] are, respectively, the resistance of electroosmosis, electrophoresis, and voltage drop at the clay/electrode interface. i_{os} and i_{ph} are determined by both R_{os} and R_{ph}. If the water content changes, R_{in} also changes. The area near the electrode is dehydrated faster, and voltage is concentrated in the area where dehydration is complete. Therefore, the potential around the electrodes is higher and the potential gradient acting on the entire clay is smaller. If there is a cohesive soil with a large R_{os} and a small R_{ph}, electroosmosis is unlikely to occur even if a large current flows through the soil. Thus, the electric current due to electroosmosis, electrophoresis, and voltage drop at the clay/electrode interface should be evaluated separately in each case study.

Figure 16 shows the results of the electroosmotic consolidation test using Kaolin clay, presented in Sect. 3.2.1, which was calculated using Eq. (2). The volume of dehydration and the change in resistance have a similar evolution over time in the case of 0.01 A. In the case of 0.02 A, R increases

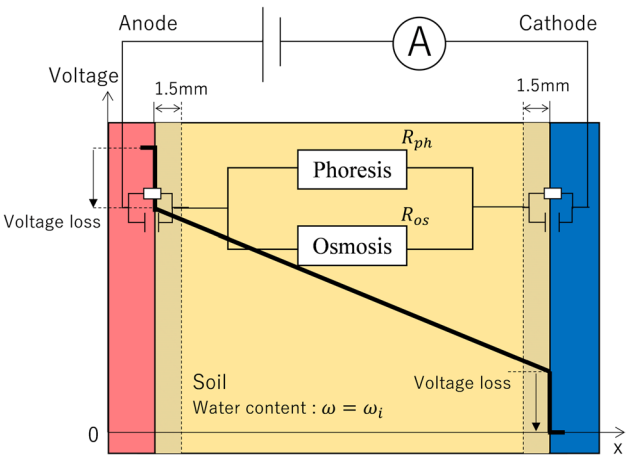

Fig. 15 Schematic diagram of electroosmotic dehydration in the clay

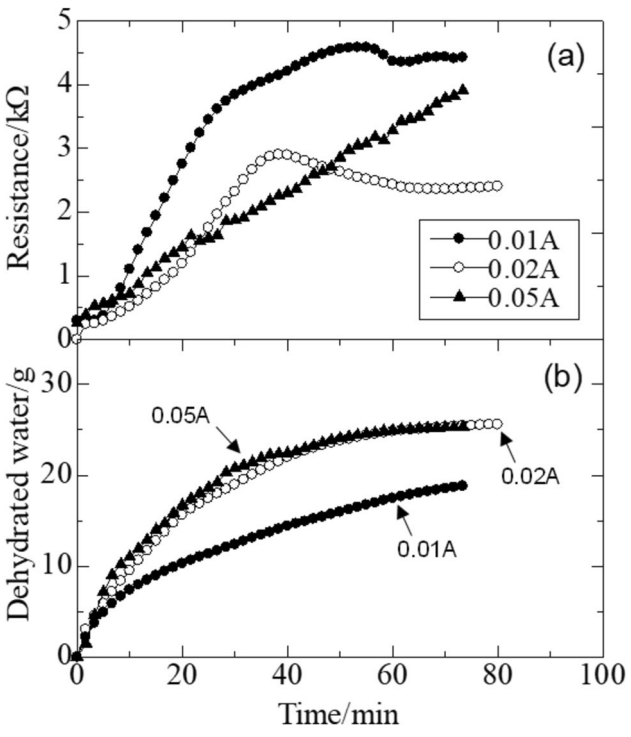

Fig. 16 The change in resistance over time (**a**) and the change in dehydrated water over time (**b**) in the case of Kaolin

steadily, and the volume of dehydration increases, while R starts to decrease after 40 min. After 70 min, both R and the volume of dehydration became constant and after 120 min, R increases again. At this time, even if R increases, the volume of dehydration does not change. Since the water content in cohesive soil is constant, R_{os} in Eq. (2) is also constant and R_{ph} should decrease due to the increase in ions in cohesive soil. Therefore, the increase in resistance R at this time is considered to be caused by electrophoresis effect. The dehydration of the pore water near the clay/electrode interface is completed at the initial stage of applying current, so the volume of dehydration does not change close to the electrode even if R_{in} increased. In the case of 0.05 A, R increases after 50 min even if the volume of dehydration becomes constant. The increase in R at this time is considered to be caused by the increase in R_{in}, as in the case of 0.02 A. Comparing the R values of each case, the dehydration is the smallest in the case of 0.01 A, although the resistance is the largest. From this, it is possible to infer that the current carriers due to electrophoresis is dominant in the case of 0.01 A, because the dehydration rate is slow and the ions in the cohesive soil have increased. As a result, R_{os} is larger than R_{ph}, which makes it difficult for electroosmosis to occur. Conversely, when comparing cases0.02 A and 0.05 A, R is large in the case of 0.05 A, although the two applied currents result in similar dehydration curves are similar. Therefore, the current i_{os} due to electroosmosis is the same in both cases, and the additional current applied in the case of 0.05 A did not improve the efficiency in this soil-electrode configuration. Instead, the increase in constant current value to 0.05 A only results in additional electrophoresis current, which does not participate in the dehydration and consolidation of the soil.

In the elemental tests using Tokyo Bay clay, experiments were conducted under constant current and constant voltage conditions. The relationships between normal dehydration and energy consumption are shown in Fig. 17. The normal dehydration is the amount calculated by dividing the amount of dehydration, which is proportional to i_{os}, by the cumulative current, which is the sum of i_{os} and i_{ph}. Since the cumulative current is the total amount of electrons produced in the anodic reaction, the normalized dehydration is the amount of water drained per unit reaction, which means the ratio of i_{os} to total current. Therefore, the larger the value of normal dehydration, the more efficiently ions are discharged and the lower the resistance to electrophoresis R_{ph}. The normal dehydration was higher in Case CV-Fe than that in Case CC-Al. This suggests that the final dehydration was higher in Case CV-Fe because of the lower R_{ph} and longer lasting electroosmosis effect.

Figure 18 shows the dehydration of Tokyo Bay clay compared to its bulk electric resistance, which is calculated using Eq. (2). In case 1 (constant current condition of 0.05 A) shown in Fig. 18a, R gradually increased until

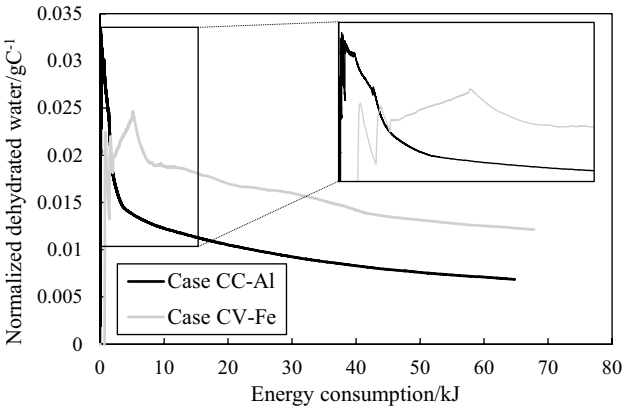

Fig. 17 The relationships between normal dehydration and energy consumption. The black and gray lines indicate the results for Case CC-Al and Case CV-Fe, respectively

130 min after applying current, decreased at the 130 min, and became constant. After 400 min, R rapidly increases, while the amount of dehydration speaks and gradually decreases. From this result, the increase in resistance R at this time is caused by an increase in R_{in}, as with kaolin clay. Since the water collection container was not covered, the amount of dehydration decreased after 600 min due to water evaporation.

In Case 2 (constant voltage condition) shown in Fig. 18b, $(R + R_{in})$ increases gradually, drops sharply after switching to the constant voltage value, and then gradually increases again. During this time, the amount of dehydration also increases, unlike in Case 1. During this stage, the change in $(R + R_{in})$ is considered to be influenced by a combination of fluctuations in R_{os}, R_{ph}, and R_{in}. After 150 min, since there is only a slight change in the amount of dehydration, excessive current is needed to increase the voltage, indicating that electrophoresis resistance is dominant over electroosmosis at this stage.

These experimental results revealed that the electroosmotic dehydration effect on cohesive soil does not increase simply by increasing the current and voltage. The electroosmotic dehydration effect can be increased by applying a current such that the electroosmotic current i_{os} is greater than the electrophoretic current i_{ph} during the test.

Furthermore, it is seen that R_{os}, R_{ph}, and R_{in} values of Kaolin clay and Tokyo Bay clay evolve differently. Since the ratio over total $(R + R_{in})$ for clay at the initial stage of applying current differs for each type of clay, the ratio of i_{os} and i_{ph} also differs depending on it. It is important to obtain these current values to control electroosmosis parameters efficiently, and it is necessary to clarify the relationship between these current ratios and the physical properties of cohesive soil.

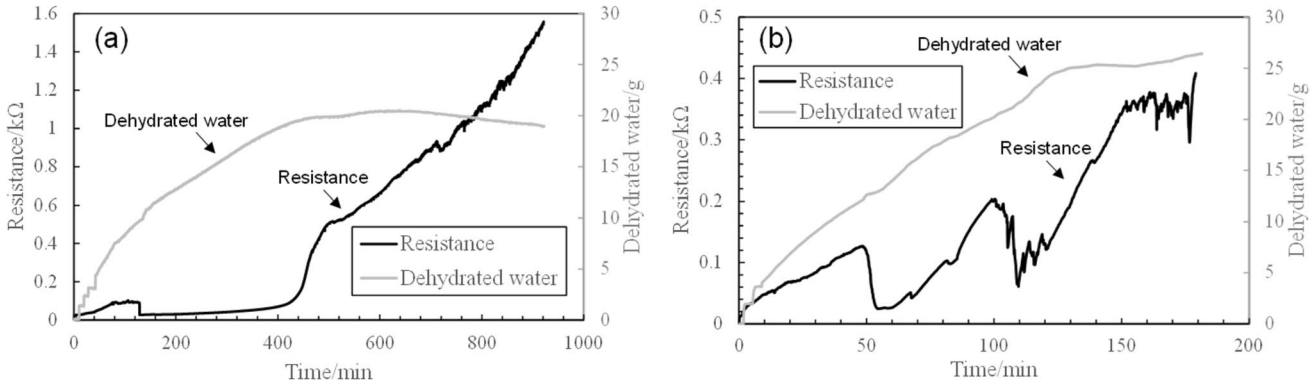

Fig. 18 The dehydration of Tokyo Bay clay compared to its bulk electric resistance ($R + R_{in}$). The results of Case CC-Al (**a**), and Case CV-Fe (**b**). The black line indicates changes in the resistance, and the red line indicates dehydrated water

4.3 Ion composition change due to the applied electric potential

The ionic composition of pore water in cohesive soil is an important factor that influences the electrochemical reaction at the clay/electrode interface, electrophoresis, electroosmosis, and cohesion of clay. From the results of EPMA analysis using the specimen after the electroosmotic consolidation test conducted in Sect. 3.3, a redistribution of ions occurred in the clay after electroosmotic dehydration. In addition, a thin oxide layer was formed by combining positive ions, migrated to the cathode side by electrophoresis, with OH^- generated at the cathode. pH increases near the cathode and decreases near the anode, resulting in uneven pH distribution in the sample. pH is closely related to zeta potential, which affects the dehydration rate. Electroosmotic dehydration effect decreases due to non-uniform pH. In order to avoid this problem, the clay needs to be dehydrated rapidly, which can limit a change in the pH inside the sample. Therefore, by minimizing the voltage drop at the clay/electrode interface and applying an electroosmosis dominant current, the pH would then be minimized and, as a result, the final dehydration volume could be increased.

5 Conclusion

In this study, three different experimental systems were developed and used to investigate three main electrochemical factors affecting the electroosmotic flow in clay soils: the voltage loss at the clay/electrode interface, the type of current carriers in the soil, and the ion composition change in the clay due to voltage application. The results can be summarized as follows:

- The polarization tests show that the voltage loss at the clay/electrode interface is different depending on the combination of the clay and electrode material. When using soil materials with low liquid resistance, such as Tokyo Bay clay, it is necessary to increase the current density in order to apply a large potential to the soil between the electrodes. In this case, the voltage drop at the clay/electrode interface has a large effect on the electroosmotic dehydration.
- The electroosmosis consolidation tests show that when a current is applied to a natural marine clay with low initial resistance, the dehydration time is three times faster under constant voltage conditions than under constant current conditions. Moreover, cations, ions moving toward the cathode due to electrophoresis, combined with OH–, generated at the cathode, form an oxide thin-film layer in the case of marine clay. This is due to its high concentration of oxidizable ions, such as sodium, as revealed by the results of EPMA analysis.
- The larger laboratory-scale electroosmotic dehydration tests, arranged in a realistic in situ layout, show that the most important factor for increasing the volume of electroosmotic dehydration is to delay shrinkage, where keeping the clay-electrode contact for a longer time period increases dehydration efficiency. When circular cracks grow faster than radial cracks, the time it takes for the clay to peel off from the wall and start shrinking becomes shorter. Conversely, when radial cracks extend faster than circular cracks, the peeling off of the clay from the cathode rod is significantly delayed.
- The relationship between bulk electric resistance of cohesive soil and current value revealed that there is an optimal current value for each cohesive soil to induce electroosmosis. During voltage application to cohesive soils, electroosmosis and electrophoresis occur simultaneously, but only electroosmosis participate to the dehydration process. Therefore, the electroosmotic dehydration effect on cohesive soil cannot be increased simply by increasing the current and voltage. However, dehydration

efficiency can be optimized by selecting a current value which maximizes electroosmotic current under specific soil and electrode conditions.

The electroosmotic consolidation test results obtained by this study, influencing the efficiency of electroosmotic consolidation, can provide additional guideline to establish improved field implementations. Furthermore, it is also required to understand the mechanical properties of the ground after electroosmotic dehydration. In future, in order to examine the application of electroosmosis to cohesive soil from a geo-mechanical point of view, the electroosmotic consolidation tests using various cohesive soils, taking into consideration the differences in the physical properties of soil materials, will be conducted. Moreover, the relationship between the zeta potential of clay and the dehydration mechanism needs to be clarified.

Acknowledgements The authors would like to thank F. Arai for technical assistance with the experiments.

Author contributions Yuri Sugiyama conceived the idea of the study and drafted the original manuscript. Yuri Sugiyama and Nagate Hashimoto developed two different experimental systems and conduct experiments. Cyrille Couture conducted image analysis of these experiments. Daiki Takano supervised the conduct of this study. All authors reviewed the manuscript draft and revised it critically on intellectual content. All authors approved the final version of the manuscript to be published.

Declarations

Conflict of interest We declare that this manuscript is original, has not been published before, and is not currently being considered for publication elsewhere. We know of no conflicts of interest associated with this publication, and there has been no significant financial support for this work that could have influenced its outcome.

References

1. Casagrande L (1949) Electroosmosis in soils. Geotechnique 1(3):159–177. https://doi.org/10.1680/geot.1949.1.3.159
2. Xue Z, Tang X, Yang Q, Wan Y, Yang G (2015) Comparison of electroosmosis experiments on marine sludge with different electrode materials. Drying Technol 33(8):986–995. https://doi.org/10.1080/07373937.2015.1011274
3. Jeyakanthan V, Gnanendran CT, Lo S-CR (2011) Laboratory assessment of electro-osmotic stabilization of soft clay. J Can Geotech 48:1788–1802. https://doi.org/10.1139/T11-073
4. Chappell BA, Burton PL (1975) Electro-osmosis applied to unstable embankment. J Geotech Eng Division ASCE 101(GT8):733–740
5. Reddy KR, Urbanek A, Khodadoust AP (2006) electroosmotic dewatering of dredged sediments: bench-scale investigation. Environ Manage 78(2):200–208
6. Lo KY, Inculet II, Ho KS (1991) Electroosmotic strengthening of soft sensitive clays. Can Geotech J 28(1):62–73. https://doi.org/10.1139/t91-007
7. Brian AC, Peter LB (1975) Electro-osmosis applied to unstable embankment. J Geotech Eng Div 101(8):733–740
8. Zareh A, Poursorkhabi RV, Majdi AA, Sarand FB (2023) The efficiency of the electro-osmosis method on the consolidation and strength properties of the gray clay of Tabriz. Geoenviron Disasters 10(1):1–12
9. Zhou J, Tao YL, Xu CJ, Gong XN, Hu PC (2015) Electro-osmotic strengthening of silts based on selected electrode materials. Soils Found 55(5):1171–1180. https://doi.org/10.1016/j.sandf.2015.09.017
10. Korolev VA, Nesterov DS (2019) Influence of electro-osmosis on physicochemical parameters and microstructure of clay soils. J Environ Sci Health Part A 54(6):570–581
11. Mahalleh HAM, Siavoshnia M, Yazdi M (2021) Effects of electro-osmosis on the properties of high plasticity clay soil: chemical and geotechnical investigations. J Electroanal Chem 880:114890. https://doi.org/10.1016/j.jelechem.2020.114890
12. Silva KN, Paiva SS, Souza FL, Silva DR, Martínez-Huitle CA, Santos EV (2018) Applicability of electrochemical technologies for removing and monitoring Pb2+ from soil and water. J Electroanal Chem 816:171–178
13. Estabragh AR, Naseh M, Javadi AA (2014) Improvement of clay soil by electro-osmosis technique. Appl Clay Sci 95:32–36
14. Liu H, Cui Y, Shen Y, Ding X (2014) A new method of combination of electroosmosis, vacuum and surcharge, preloading for soft ground improvement. China Ocean Eng 28(4):511–528. https://doi.org/10.1007/s13344-014-0042-3,ISSN0890-5487
15. Karunaratne GP (2011) Prefabricated and electrical vertical drains for consolidation of soft clay. Geotext Geomembr 29:391–401
16. Bo MW, Choa V, Zeng XQ (2001) Laboratory investigation on electroosmosis properties of Singapore marine clay. Soils Found 41(5):15–23
17. Chew SH, Karunaratne GP, Kuma VM, Lim LH, Toh ML, Hee AM (2004) A field trial for soft clay consolidation using electric vertical drains. Geotext Geomembr 22(1–2):17–35. https://doi.org/10.1016/S0266-1144(03)00049-9
18. Mohamedelhassan E, Shang JQ (2002) Feasibility assessment of electro-osmotic consolidation on marine sediment. Proc ICE Ground Improvement 6(4):145–152. https://doi.org/10.1680/grim.2002.6.4.145
19. Shang JQ, Lo KY, Huang KM (1996) On factors influencing electro-osmotic consolidation. Geotech Eng 27(2):23–26
20. El Naggar MH, Routledge SA (2004) Effect of electro-osmotic treatment on piles. Proc ICE Ground Improvement 8(1):17–31. https://doi.org/10.1680/grim.2004.8.1.17
21. Zhuang YF (2021) Large scale soft ground consolidation using electrokinetic geosynthetics. Geotext Geomembr 49(3):757–770. https://doi.org/10.1016/j.geotexmem.2020.12.006
22. Hu L, Wu W, Wu H (2012) Numerical model of electroosmotic consolidation in clay. Geotechnique 62(6):537–541
23. Lewis RW, Garner RW (1972) A finite element solution of coupled electrokinetic and hydrodynamic flow in porous media. Int J

Numer Meth Eng 5(1):41–55. https://doi.org/10.1002/nme.1620050105
24. Mohamedelhassan E, Shang JQ (2001) Analysis of electrokinetic sedimentation of dredged Welland River sediment. J Hazard Mater 85(1–2):91–109. https://doi.org/10.1016/S0304-3894(01)00223-0
25. Yuan J, Hicks MA (2015) Numerical analysis of electro-osmosis consolidation: a case study. Géotech Lett 5(3):147–152. https://doi.org/10.1680/jgele.15.00045
26. Zhuang YF, Wang Z (2007) Interface electric resistance of electroosmotic consolidation. J Geotech Geoenviron Eng 133(12):1483–1640. https://doi.org/10.1061/(ASCE)1090-0241(2007)133:12(1617)
27. Yang S, Jianting F, Wen S, Chenchen Q (2019) Effects of voltage gradients on electro-osmotic characteristics of Taizhou soft clay. Int J Electrochem Sci 14:2136–2159. https://doi.org/10.20964/2019.03.06
28. Sugiyama Y, Takano D, Morikawa Y (2022) Study on volume reduction method for dredged soil by electroosmosis-An investigation into applicability of electroosmosis in clays-, Technical note of the port and airport research institute, No.1404, ISSN: 1346-7840
29. ASTM, 2020. Standard Test Method for One-Dimensional Consolidation Properties of Soils Using Incremental Loading. D2435. American Society for Testing and Materials, Philadelphia PA, USA.
30. JSCE-G574-2013: Plane Analysis Method of Elements in Concrete by EPMA Method, 2013 Concrete Standard Specifications, Japan Society of Civil Engineers Criteria and Related Criteria, Japan Society of Civil Engineers, pp.387–400.
31. JIS K 0102:2019: Detailed factory wastewater test method
32. The Standard Methods of Analysis for Mineral Springs (2014), The Ministry of Environment, pp. 79–85, in Japanese.